



# LUND UNIVERSITY

## Dynamics of Polymer Adsorption onto Solid Surfaces in Good Solvent

Källrot, Niklas

2009

[Link to publication](#)

*Citation for published version (APA):*

Källrot, N. (2009). *Dynamics of Polymer Adsorption onto Solid Surfaces in Good Solvent*. [Doctoral Thesis (compilation), Physical Chemistry]. Lund University (Media-Tryck).

*Total number of authors:*

1

### General rights

Unless other specific re-use rights are stated the following general rights apply:

Copyright and moral rights for the publications made accessible in the public portal are retained by the authors and/or other copyright owners and it is a condition of accessing publications that users recognise and abide by the legal requirements associated with these rights.

- Users may download and print one copy of any publication from the public portal for the purpose of private study or research.
- You may not further distribute the material or use it for any profit-making activity or commercial gain
- You may freely distribute the URL identifying the publication in the public portal

Read more about Creative commons licenses: <https://creativecommons.org/licenses/>

### Take down policy

If you believe that this document breaches copyright please contact us providing details, and we will remove access to the work immediately and investigate your claim.

LUND UNIVERSITY

PO Box 117  
221 00 Lund  
+46 46-222 00 00



# Dynamics of Polymer Adsorption onto Solid Surfaces in Good Solvent

Niklas Källrot



LUND UNIVERSITY

**Doctoral Thesis**

The thesis will be publicly defended on Friday 13th of November 2009,  
10.30 in lecture hall C, Center for Chemistry and Chemical  
Engineering, Lund

The faculty opponent is Prof. Dr. Martien A. Cohen Stuart from the  
Scientist Laboratory of Physical Chemistry and Colloid Science,  
department of Agrotechnology and foodsciences at the Wageningen  
University.

© Niklas Källrot 2009  
Doctoral Thesis

Physical Chemistry  
Chemical Center for Chemistry and Chemical Engineering  
Lund University  
P.O. Box 124  
SE-221 00 Lund  
Sweden

*All rights reserved*

ISBN 978-91-7422-233-3  
Printed by Mediatryck, Lund University, Lund

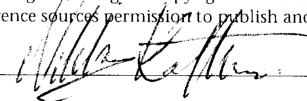
# Dynamics of Polymer Adsorption onto Solid Surfaces in Good Solvent

Organization LUND UNIVERSITY  Physical Chemistry Centre for Chemistry and Chemical Engineering P.O. Box 124, SE-221 00. Lund. Sweden	Document name DOCTORAL DISSERTATION	
	Date of issue November 13, 2009	
	Sponsoring organization  Faculty of Science Lund University	
Author(s) Niklas Källrot		
Title and subtitle Dynamics of Polymer Adsorption onto Solid Surfaces in Good Solvent		
Abstract <p>Adsorption dynamics of various types of uncharged homopolymers onto solid surfaces in good solvent have been studied by using a coarse grained bead-spring model. Brownian dynamics simulation has been used to examine the adsorption process for polymers released near an adsorbing surface, and Monte Carlo simulations have been employed to explore equilibrium properties of adsorbed polymers.</p> <p>Two different types of approaches have been pursued: adsorption of single polymers and adsorption from polymer solutions. For single polymers of varying type, the entire adsorption process was examined and characteristic time dependent properties were extracted. Structural rearrangements of the polymers comprising time regimes of several orders of magnitude were identified. Regarding polymer solutions, polymers of varying length, flexibility, and surface attraction were examined for solutions of similar and dissimilar polymer types at different densities. Solutions containing flexible polymers revealed an extension perpendicular to the surface at long times as the surface pressure increases, reducing the adsorbed polymer segment fraction. Systems of rod-like polymers display an additional relaxation mode, prolonging the final stage of the adsorption process due to the formation of nematic structures of polymers on the surface. Finally, the competitive adsorption of mixed polymer systems is characterized by an initial adsorption of both polymer types, followed by a slow exchange at the surface as the preferentially adsorbing polymer type replaces the other one.</p>		
Key words: molecular modeling, Brownian dynamics, single chain, polymer adsorption, competitive adsorption, conformational relaxation		
Classification system and/or index terms (if any):		
Supplementary bibliographical information:	Language English	
	ISBN 978-91-7422-233-	
Recipient's notes	Number of pages 172	Price
	Security classification	

Distribution by (name and address)

I, the undersigned, being the copyright owner of the abstract of the above-mentioned dissertation, hereby grant to all reference sources permission to publish and disseminate the abstract of the above-mentioned dissertation.

Signature



Date 2009 10 01

# List of Papers

This thesis is based on the following papers, which will be referred to in the text by their Roman numerals. The papers are appended at the end of the thesis.

**I Dynamic Study of Single-chain Adsorption and Desorption**

Niklas Källrot and Per Linse

*Macromolecules*, 40 4669-4679 **2007**

**II Dynamics of Polymer Adsorption from Bulk Solution onto Planar Surfaces**

Niklas Källrot, Martin Dahlgqvist, and Per Linse

*Macromolecules*, 42 3641-3649 **2009**

**III Polymer Adsorption from Bulk Solution onto Planar Surfaces: Effect of Polymer Flexibility and Surface Attraction in Good Solvent**

Per Linse and Niklas Källrot

*submitted to The Journal of Physical Chemistry B*

**IV Dynamics of Competitive Polymer Adsorption onto Planar Surfaces in Good Solvent**

Niklas Källrot and Per Linse

*submitted to The Journal of Physical Chemistry B*

Other Papers (not included in this thesis):

- **Theoretical study of structure of catalytic copper site in nitrite reductase**

Niklas Källrot, Kristina Nilsson, Torben Rasmusson, and Ulf Ryde  
*Int. J. Quantum Chem.*, 102, 520-541, **2005**

- **Formation of a New  $Ia_3d$  Cubic Meso-Structured Silica via Triblock Copolymer-Assisted Synthesis**

Katarina Flodström, Viveka Alfredsson, and Niklas Källrot  
*J. Am. Chem. Soc.*, 125, 4402-4403, **2003**



# Tackord

Jag vill först och främst tacka dig, **Per Linse** för att du erbjöd mig en chans att få driva ett forskningsprojekt tillsammans med dig. Jag har aldrig träffat någon så intelligent och strukturerad människa som du och det har varit oerhört lärorikt att angripa diverse problemställningar tillsammans med dig. Bitvis har det varit en tuff resa för oss båda, men med facit i hand är jag mycket nöjd och stolt över det vi åstadkommit tillsammans.

Under min tid som doktorand i Lund har jag träffat en mängd intressanta och roliga personer. Jag vill därför ta tillfället i akt att tacka några av dem som har gjort det lättare att gå till jobbet även de dagar när forskningen har tagit emot. Bland dessa finns:

**Peter Linton**, en hårt arbetande småbarnsfar med sinne för humor och diplomati. Du har varit ett stort stöd under tunga perioder och en ändlös källa till vänskap och skratt. Jag kan inte riktigt se att jag hade hållit hela vägen om du inte hade varit medresenär.

**David Löf**, studiekamrat under nästan hela grundutbildningen och senare även kontorskamrat - imponerande envis och målinriktad när det gäller. Du har varit en tillgång med ditt starka driv på alla kurser vi läst ihop. Jag har alltid uppskattat din uppriktighet och din sjuka humor.

**Lars Nilsson**, den i särklass mest kunniga kemisten i min egen ålder och en riktig uppesittare på After-Work. Lars, du är en ung, framgångsrik forskare helt enkelt och du får mig alltid att skratta riktigt högt, tack för det.

**Marie-Louise Ainalem**, ambitiös som få, både i labbet och på fritiden. Du är en riktig pärla med ett beundransvärt tålamod i alla situationer. Dina balanserade inlägg i debatten är uppfriskande.

**John Janiak**, det har varit kul att ha dig på kort avstånd, beredd att slänga käft över en kaffe precis när som helst, du är alltid rak och ärlig vilket jag uppskattar mycket.

**Joakim Stenhammar**, du har varit ett bra hårdvarustöd och en sund röst i förhandlingar med de styrande elementen på KC, stå på dig bara, skam den som ger sig.

På kontoret, där flitens lampa tidvis lyst starkt, vill jag tacka:

**Agnes Zettergren**, en flitig dam med skinn på näsan som har hjälpt till att hålla sarkasmen på en jämn och hög nivå inne på kontoret. Det har alltid varit en bra start på dagen att få ta en kopp kaffe med dig. Du tror kanske inte att det märks, men jag vet i alla fall att du har ett hjärta av guld.

**Sebastian Björklund**, ett sent tillskott och ovanlig syn på kontoret som briljerar i det mesta han tar sig för. Du har ett behagligt lugn över dig som har bidragit med en skön stämning. Tack för alla trevliga avbrott i arbetet och för musiken.

**Jimmy Heimdal**, frekvent besökare och hedersgäst på kontoret. Du skall även ha ett tack för att du varit en god studiekamrat på tiden när det begav sig.

Vidare vill jag passa på att tacka **Majlis Larsson** för att du är så omtänksam och hjälpsam, **Christoffer 'junior' Åberg** för hjälp med diverse matematiska spörsmål och formatteringsfrågor i L<sup>A</sup>T<sub>E</sub>X, **Magnus Ullner** för att du alltid har tagit dig tid, och **Lennart Piculell**, tack för råd och samtal av icke-kemisk natur. Jag vill också tacka **Martin Dahlqvist** för ett bra samarbete under ditt ex-jobb.

Utanför institutionen, men fortfarande med anknytning till ämnet finns:

**Peter Sellers** som bidragit med språkgranskning av både artikel och avhandling. Tänk att det hela började med att du hjälpte mig med kemin på gymnasiet. Tillsammans med **Pia** har ni båda varit ett stort stöd och jag värderar er vänskap och ert omdöme högt, tack.

**Marie Skepö**, som agerat mentor och god vän. Ditt stöd har varit ovärderligt under min tid som doktorand och du får mig alltid att känna mig hoppfull inför morgondagen. Tack för att du tog mig under din vinge.

Det kan verka främmande för vissa, men det finns folk utanför universitetets tjocka ringmur också, jag skulle vilja nämna några av de bästa: Stort tack till **Hajro** för din trofasta vänskap och dina djupa psykoanalyser, **Oskar** för den ändlösa jakten på perfekta surf-spots och **Johan** för bastu- och videokvällar samt för att du håller ihop hela gänget.

**Anders** och **Bibbi** vill jag tacka för all uppmuntran, men framförallt för att ni alltid tar så väl hand om mig. Linköping har blivit min främsta kurort under de sista åren.

Jag vill tacka mina föräldrar **Magnus** och **Suzanne** för att ni alltid ställer upp och tror på mig, vad jag än hittar på. Mina båda systrar, **Alexandra** och **Johanna** vill jag tacka för ert orubbliga stöd i alla situationer och för att ni alltid delar med er. Det är en enorm trygghet att veta att ni alla finns till hands och att ni bevakar mina intressen så starkt.

Sist men inte minst vill jag tacka den som får mig att vilja gå till jobbet bara för att jag får komma hem till henne igen, **Clara**. Din kärlek är min drivkraft.



# Contents

<b>1</b>	<b>Introduction</b>	<b>1</b>
<b>2</b>	<b>Polymers in Solution</b>	<b>3</b>
2.1	Classifications . . . . .	3
2.2	The Single Chain . . . . .	5
2.3	The Extension of a an Ideal Chain . . . . .	6
2.4	Chain Expansion and Solvent Conditions . . . . .	8
2.5	Properties of the Solution . . . . .	9
<b>3</b>	<b>Polymer Adsorption</b>	<b>11</b>
3.1	Simple Description . . . . .	11
3.2	Obtaining Adsorption Isotherms . . . . .	14
<b>4</b>	<b>Modelling of Polymers</b>	<b>15</b>
4.1	Coarse Graining . . . . .	15
4.2	General Approach . . . . .	16
4.3	Polymer Interaction Potentials . . . . .	16
4.4	External Interaction Potentials . . . . .	18
<b>5</b>	<b>Statistical Thermodynamics</b>	<b>21</b>
5.1	The Boltzmann Distribution and Entropy . . . . .	21
5.2	Classical Statistical Mechanics . . . . .	22
<b>6</b>	<b>Molecular Simulation Techniques</b>	<b>25</b>
6.1	Motivation . . . . .	25
6.2	Monte Carlo Simulation . . . . .	26
6.3	Brownian Dynamics Simulation . . . . .	27
6.4	Boundary conditions . . . . .	28
6.5	Truncation and Neighbor Lists . . . . .	29
6.6	Simulation Protocol . . . . .	31
6.7	Sampled Properties . . . . .	32

<b>7 Highlights of the Papers</b>	<b>37</b>
7.1 Paper I . . . . .	37
7.2 Paper II . . . . .	38
7.3 Paper III . . . . .	39
7.4 Paper IV . . . . .	40
 Populärvetenskaplig sammanfattning på svenska	 41

# Chapter 1

## Introduction

Polymer adsorption is a phenomenon which is of great importance in a number of areas in our everyday life. In many technical applications, understanding and controlling polymer adsorption onto solid surfaces is essential to the outcome of a product. Such technical areas may comprise formulations of drugs, paints, detergents, cosmetics, and food stabilizers. Biological aspects include mapping the adsorption of biopolymers, such as mucin in the saliva or other proteins, to determine their structure and function. Needless to say, the area of research is quite large and well developed already. Numerous techniques for determining polymer surface layer thickness and surface structure exist. However, there are still many gaps to fill concerning the time-dependent properties of polymer adsorption. With modern technology, the probed length- and time scales gradually become smaller, motivating and enabling a deeper understanding of surface phenomena on a detailed molecular level.

Using computer simulations in the field of polymer adsorption is no new approach; the mathematically descriptive nature of polymers led to various early numerical calculations. The vast technological advances in computer science allow us to explore increasingly more complex issues and systems. Using simulations, as in the work presented here, time-dependent properties are resolved which are related to the interaction between different types of polymers and surfaces. These calculations need not be very complicated, but the number of numerical operations needed to realize the motion of a polymer solution is enormous.

As a polymer adsorbs onto a surface, there is an associated loss in conformational entropy. This loss in entropy must be smaller than the energetic gain in enthalpy for the polymer upon adsorbing onto the surface. If the interaction with the surface is strong the adsorbed polymers will attain flatter conformations than if there is a weak interaction.

The degree of interaction between a polymer and a surface may be modified in several ways. The monomer-surface interaction strength and the characteristics of the polymer, such as size and flexibility, have a significant impact on the degree of adsorption. Other properties which influence the behavior are the density and composition of the polymer solution. The entire adsorption process of a polymer is a continuous transition from a three-dimensional state in solution to the final equilibrium two-dimensional-like structure at the surface. The full transition covers time regimes of several orders of magnitude, and the pathway toward equilibrium may vary depending on the properties of the polymer. In mixed solutions of different polymer types, the relaxation process is prolonged due to competitive effects in the vicinity of and on the surface.

The immediate applications of the knowledge gained in this work are of course not evident. The study which is presented here is but a small contribution to the growing understanding of polymer adsorption. However, novelty lies in the method with which we conduct our study, along with the qualitative results we gain in employing this. We thus feel that this work is a valuable contribution to the field.



## Chapter 2

# Polymers in Solution

### 2.1 Classifications

A polymer is defined by its repetitive structural units of lower molecular weight which are connected to one another creating a larger entity with a high relative molecular weight. Because of the (often) large size of the formed entities, polymers are frequently referred to as macromolecules. Polymers consisting of identical repeating monomers are called *homopolymers*. If units or blocks of monomers of different species are combined in a repeating fashion, these are named *block copolymers* and if different units are connected in a completely random fashion these are called *heteropolymers*. Furthermore, any of the above classifications can also be referred to as a *polyelectrolyte* if the polymer carries ionizable units. Schematic figures of some different polymer types are given in Figure 2.1 below.

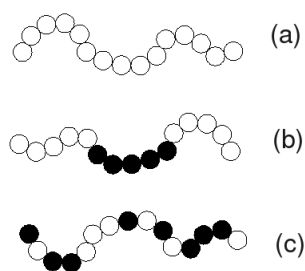


Figure 2.1: Classes of polymers which depend on the physical relation of the monomeric composition of a polymer, (a) homopolymer, (b) block copolymer, and (c) heteropolymer.

The subunits or monomers in a polymer may of course be connected together in a number of different ways as shown in Figure 2.2. Besides the most intuitive *linear* structure, there are various types of branched polymers such as *comb*, *star*, *randomly branched*, and *polymer networks*.

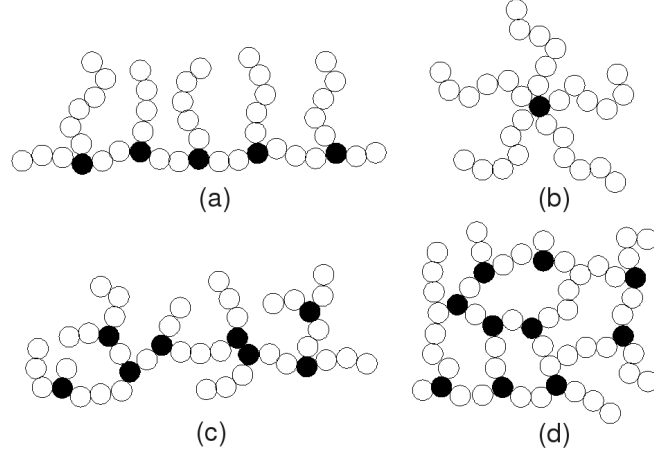


Figure 2.2: Different branched polymer structures: (a) comb, (b) star (c) randomly branched, and (d) polymer network, where the junction monomers are indicated (black).

Polymers are formed by stepwise linking together the monomers  $N_b$  of which it is made up

$$N_{b,n} + N_b \rightarrow N_{b,n+1} \quad (2.1)$$

For monomers of a singular given molecular weight  $M_b$ , the total molecular weight  $M_p$  of a polymer consisting of  $N$  monomers is given by

$$M_p = NM_b \quad (2.2)$$

The total number of monomers  $N_b$  which comprise a given polymer may vary by orders of magnitude, from  $N_b \sim 10^2 - 10^4$  for synthetic polymers up to  $N_b \sim 10^9 - 10^{10}$  for natural polymers, such as DNA.<sup>1</sup> Often for synthetic polymers, along with some biological ones, the reaction which successively builds the macromolecule is end-terminated at

different positions along the chain. This causes polymers to vary greatly in molecular weight, and one is often interested in the weight distribution,  $p(M)$ , among the polymers in a sample rather than the number of monomers of each polymer. The degree of polymerization or *number average*,  $\langle M_n \rangle$ , for a discrete distribution of molecular weights of a polymer type can be expressed as the probability,  $p(M_i)$ , of finding a molecular weight  $M_i$ , summed over all polymers in a sample

$$\langle M_n \rangle = \sum_i p(M_i) M_i \quad (2.3)$$

where the following condition  $\sum_i p(M_i) = 1$  is met. The *weight average*,  $\langle M_w \rangle$ , is similarly

$$\langle M_w \rangle = \frac{\sum_i p(M_i) M_i^2}{\sum_i p(M_i) M_i} \quad (2.4)$$

The ratio between the molecular weight average and the molecular number average

$$D_M = \frac{\langle M_w \rangle}{\langle M_n \rangle} \quad (2.5)$$

is called *molar mass dispersity*, or is often referred to as *polydispersity index* and is a measure of the width of the distribution of molecular weights in a sample. For a uniform polymer solution (monodisperse), the molar mass dispersity is unity, and for any other non-uniform polymer solution it is larger than unity.

A polymer immersed in a solvent will adopt a three-dimensional conformation in relation to its chemical composition and interaction with its surroundings. If the thermal fluctuations of the solvent at equilibrium are of higher energy than the rigidity of the polymer backbone in terms of rotation about bonds, the polymer is considered *flexible*.

## 2.2 The Single Chain

Any single small particle suspended in a solvent will be continuously subjected to collisions from the surrounding solvent molecules. This is

known as Brownian motion and will cause the particle to diffuse through the media in a non-deterministic fashion. If the erratic path of a single particle was traced during some time interval, it would well describe a random walk, which is a fundamental mathematical description of a polymer. For a more thorough introduction to single chain statistics, see one of the textbooks on the subject.<sup>1-4</sup>

### 2.3 The Extension of a an Ideal Chain

Assuming no interaction between segments which make up the chain, a polymer may be considered as a sequence of  $N$  completely randomly distributed segments (i.e random walk) as depicted in Figure 2.3. This is then referred to as an *ideal chain*.

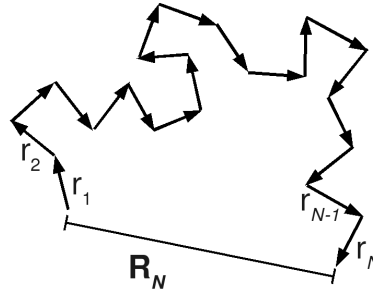


Figure 2.3: Illustration of the random walk model in two dimensions.

The bond-vector for the  $i$ th segment is thus  $\mathbf{r}_i$ , and the full extension of the chain, which is the end-to-end vector for the complete set of segments  $\mathbf{R}_N$ , is described by

$$\langle \mathbf{R}_N^2 \rangle = \left\langle \left| \sum_{i=1}^N \mathbf{r}_i \right|^2 \right\rangle \quad (2.6)$$

The *freely jointed chain* is an ideal chain with  $N$  discrete segments of length  $\ell$ , and its extension is thus given by

$$R_N \equiv \langle \mathbf{R}_N^2 \rangle^{1/2} = N^{1/2} \ell \quad (2.7)$$

In the limit that  $\ell \rightarrow 0$  and  $N \rightarrow \infty$  along with an assumption of no rotational angle between consecutive segments for a chain at fixed contour length  $L$ , we obtain the *wormlike chain* as a continuous ideal chain. The end-to-end vector for the wormlike chain then becomes

$$\mathbf{R}_N = \int_0^L \mathbf{l}(s) ds \quad (2.8)$$

where  $\mathbf{l}(s) = \partial \mathbf{r} / \partial s$  is the unit vector of a chain direction at distance  $s$  from the start of the chain along its contour. Furthermore, from eq 2.7 we find a scaling relation between the end-to-end distance and the number of segments or length of a polymer,  $\langle R_N \rangle \sim N^{1/2}$ .

For all polymers there exists a length at which individual segments may be considered as stiff, and the segmental contour length can be regarded as having roughly the same size as the segments end-to-end distance. This is referred to as a Kuhn segment, and relates the individual flexibility of a polymer to its average extension. To quantify this, we define the persistence length  $l_p$  as the distance over which the memory of a polymers direction is retained,

$$\langle \cos \theta(s) \rangle = e^{-\frac{s}{l_p}} \quad (2.9)$$

where  $\theta(s)$  is the average intersecting angle between tangents at the end points of a Kuhn segment  $s$ .

Another useful property which describes the extension of a polymer in three dimensions is the radius of gyration,  $R_g$ , which is defined according to

$$\langle R_g^2 \rangle = \left\langle \frac{1}{N} \sum_{i=1}^N [\mathbf{r}_i - \mathbf{r}_{com}]^2 \right\rangle \quad (2.10)$$

with the center of mass

$$\mathbf{r}_{com} = \frac{1}{N} \sum_{i=1}^N \mathbf{r}_i \quad (2.11)$$

where  $\mathbf{r}_i = [x_i, y_i, z_i]$  is the coordinate of segment  $i$ . The relation between the radius of gyration and the end-to-end distance is given by

$$\langle R_g^2 \rangle = \frac{\langle R_N^2 \rangle}{6} = \frac{N\ell^2}{6} \quad (2.12)$$

If we represent a polymer by a collection of volumeless points connected by vectors, the probability distribution of the end-to-end vector can be described by a *Gaussian* function in the limit  $N \rightarrow \infty$

$$P(\mathbf{R}_N) = \left( \frac{3}{2\pi N\ell^2} \right)^{-\frac{3}{2}} \exp \left( -\frac{3\mathbf{R}_N^2}{2N\ell^2} \right) \quad (2.13)$$

where the distribution is normalized so that the sum over all values of  $\mathbf{R}_N$  gives a probability of one. A polymer which can be described by such statistics is often referred to as a *gaussian chain*.

## 2.4 Chain Expansion and Solvent Conditions

A more realistic model of a polymer than that of the random walk can be obtained by including a self-volume of the segments or monomers that make up the chain; in other words, by restricting the space available to segments due to *excluded volume* interactions between sections of the polymer. The simplest way of approaching this is by using the self-avoiding walk (SAW), in which a polymer segment is forbidden to occupy the same space as previously visited during the same walk. A self-avoiding walk in three dimensions will cause the polymer chain to expand, and computer simulations show a scaling behavior with respect to the end-to-end distance of  $\langle R_N \rangle \sim N^\nu$ , where the Flory exponent  $\nu \approx 3/5$  for large  $N$ .

The randomness in the walks discussed above originates from the intrinsic properties of the solvent in which a polymer is immersed. The extension of a single polymer in solution as we have concluded so far comes from the random walk and the excluded volume interactions between segments of the chain. The mathematical formulation of the random walk and self avoiding walk discussed is referred to as *athermal*, which implies no influence of temperature, though it is implicitly present by the origin of random walk (motion) in our model.

From regular solution theory temperature can explicitly be included in the model via an energy term  $\chi$ , which describes the interaction between a monomer and its surroundings. The net difference in interacting with a non-adjacent segment or interacting with a solvent molecule for a given polymer segment determines the sign and magnitude of this parameter. Furthermore,  $\beta = 1/k_B T$ , where  $k_B$  is the Boltzmann constant, is included in the parameter, making this dimensionless and inversely proportional to the temperature  $T$ . Thus the random excursions (expansion) of a polymer and the energy minimization of segment interaction (contraction) determine the extension of a polymer in solution. For different values of the  $\chi$ -parameter a polymer will adopt characteristic conformations according to<sup>5</sup>

- *Good solvent conditions*,  $\chi < 0.5$ , where the expansion of the polymer dominates. A polymer behaves according to the SAW-model.
- *Bad solvent conditions*,  $\chi > 0.5$ , where segment–segment interactions are strong and contraction of the polymer prevails.
- *$\theta$  solvent conditions*,  $\chi = 0.5$ , at which a polymer will behave as a gaussian chain discussed above. The temperature at which this occurs is referred to as the  $\theta$  temperature

One can now show a relation between the  $\chi$ -parameter and the Flory exponent  $\nu$ , which relates the scaling behavior of the extension of a polymer to its interaction in a solvent.

## 2.5 Properties of the Solution

In a polymer solution of finite concentration  $c$  the interaction between different polymers must be taken into account. Depending on the nature of a polymer type, the polymers in a solution may start to interpenetrate and overlap at relatively low polymer concentrations. Consequently there exists three concentration regimes of polymer solutions which are displayed in Figure 2.4, and are referred to as: (i) *dilute*, where polymers may be treated as isolated, (ii) *semidilute*, where polymers interact and, (iii) *concentrated*, where substantial interaction at a high polymer volume fraction takes place. The crossover from a dilute to a semidilute solution is characterised by the *overlap concentration*,  $c^*$ . The overlap concentration may be estimated as the concentration when the total volume

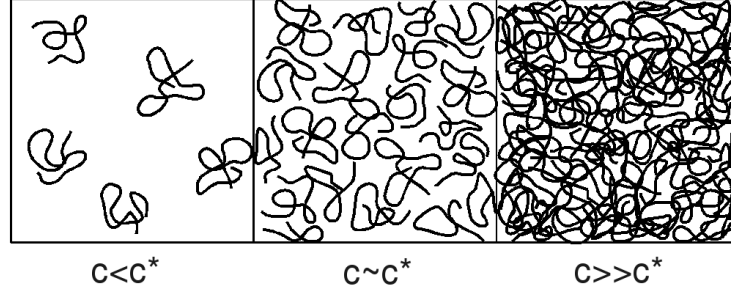


Figure 2.4: The three concentration regimes in relation to the overlap concentration  $c^*$

of polymers is comparable to that of the volume available to the solution. The onset of  $c^*$  is well defined, but the transition at the overlap concentration is of continuous nature.

For polymers in a dilute solution, these may diffuse as isolated entities unperturbed by other polymers. The translational self-diffusion of a polymer coil may then be described by the Stokes-Einstein relation

$$D = \frac{k_B T}{6\pi\eta r} \quad (2.14)$$

where  $\eta$  is the solvent viscosity and  $r$  the radius of the polymer coil. In a  $\theta$  solvent the self-diffusion coefficient dependence of the molecular weight  $M$  is  $D \sim M^{-0.5}$ .

In a semidilute solution, the translational motion of a polymer is hindered by the presence of neighboring polymers and diffusion may only be realized through *reptational* motion in the surrounding mesh of polymers. This gives  $D \sim M^{-2}$  as the relation between the diffusion coefficient and the molecular weight. Thus polymer diffusion depends significantly on the concentration and the molecular weight.



## Chapter 3

# Polymer Adsorption

Polymer adsorption is classified in accordance to the nature of interaction between polymer and surface. If the interaction energy is considerable (two or more orders of magnitudes larger than  $k_B T$ ), covalent bonds may form between the polymer and surface making the adsorption irreversible. This type of adsorption is referred to as *chemisorption*. If on the other hand the attraction is weak or moderate (in the order of  $k_B T$ ) the adsorption is less rigid and is then referred to as *physisorption*. Chemisorption is often a slow process associated with a much higher energy barrier than that of the faster, often diffusion controlled physisorption.<sup>6</sup> In this work we are concerned only with physisorption of polymers to solid surfaces.

The adsorption process of a polymer to a surface may be expressed as a step-wise process involving: (i) a diffusion toward the surface, (ii) an attachment to the surface, and (iii) a spreading on the surface. In the following section we derive an expression for the adsorption rate of a solution of one adsorbing component and try to relate this to processes (i) and (ii). Further descriptions of the theories of adsorption and adsorption kinetics may be found in a number of textbooks and reviews exist.<sup>5,7-12</sup>

### 3.1 Simple Description

For simplicity we consider the adsorption of small molecules which do not deform upon adsorption to a surface. We further assume a situation of steady-state convective diffusion with a linear concentration gradient, which governs the transport of molecules to the surface from bulk. This flux,  $J$ , is then directly related to the adsorption rate  $d\Gamma/dt$ , and defined as

$$J = k(c_b - c_s) \quad (3.1)$$

where  $k$  is the rate constant dependent on the hydrodynamic conditions of the solvent and diffusion coefficient, and  $c_b$  along with  $c_s$  are the solute concentrations of the bulk and in the surface region, respectively. Molecules in the vicinity of the surface may attach to it and molecules which are adsorbed may detach from the surface. This gives rise to a flux in each direction and the net flux describes the adsorption rate via

$$\frac{d\Gamma}{dt} = \left. \frac{d\Gamma}{dt} \right|_+ - \left. \frac{d\Gamma}{dt} \right|_- \quad (3.2)$$

The positive flux is dependent on the attachment rate constant  $k_a$ , the solute concentration at the vicinity of the surface, and the available surface fraction  $\theta$  according to

$$\left. \frac{d\Gamma}{dt} \right|_+ = k_a(1 - \theta)c_s \quad (3.3)$$

where the surface fraction is defined as  $\theta \equiv \Gamma/\Gamma_{max}$ , and  $\Gamma_{max}$  represents the maximum adsorbed amount at saturation. Assuming no deformation of adsorbed species this is a valid definition. The negative flux is defined as

$$\left. \frac{d\Gamma}{dt} \right|_- = k_d\theta \quad (3.4)$$

where  $k_d$  is the rate constant associated with the desorption.

As the surface coverage increases, the negative flux increases as well until steady-state conditions are met where the net flux in eq 3.2 is zero, corresponding to

$$k_a(1 - \theta)c_{eq} = k_d\theta \quad (3.5)$$

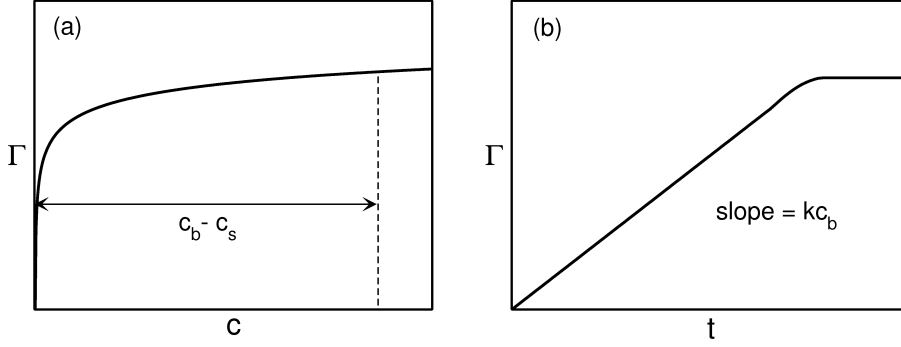


Figure 3.1: (a) Typical high-affinity adsorption isotherm, and (b) the corresponding kinetic curve, inspired by figures in ref.<sup>13</sup>

This gives an expression for the net adsorption rate

$$\frac{d\Gamma}{dt} = \left. \frac{d\Gamma}{dt} \right|_+ - \left. \frac{d\Gamma}{dt} \right|_- = k_a(1 - \theta)(c_s - c_{eq}) \quad (3.6)$$

Now using the expression for the adsorption rate in eq 3.1 combined with the derived expression of the net adsorption rate at steady-state in eq 3.6, we obtain a general adsorption rate equation

$$\frac{d\Gamma}{dt} = \frac{c_b - c_{eq}}{\frac{1}{k} + \frac{1}{k_a(1-\theta)}} \quad (3.7)$$

The equilibrium concentration  $c_{eq}$  is dependent on the equilibrium adsorbed amount  $\Gamma$ . Hence, to obtain an explicit expression of the adsorption rate  $d\Gamma/dt$ , an adsorption isotherm for  $c_{eq}(\Gamma)$  is needed. This involves a description of the interaction between the adsorbing molecules, solvent, and surface. Such predictions have been developed using *self-consistent field* theories,<sup>13</sup> which give important information of the adsorbed fraction as a function of the density profile of the polymers at the surface.<sup>14</sup>

The use of the formulation above (eq 3.7) shows that for an attachment process which is unhindered i.e.,  $k_a \gg 1$ , the expression can be used to predict the adsorption rate from the equilibrium adsorption isotherm. Given the isotherm of a typical high-affinity polymer, one finds that  $c_{eq} \simeq 0$  up to almost saturation<sup>9</sup> (Figure 3.1a). This gives a linear

behavior between the diffusion controlled transport and the adsorption rate, which is the highest rate of adsorption for the polymers and is known as the limiting flux,  $J_0$ .<sup>11</sup> Knowing the adsorption isotherm and thus the function  $c_{eq}(\Gamma)$  we may solve the differential equation for  $\Gamma(t)$  and construct a kinetic curve of the adsorption process. An initial linear increase in the adsorption as a function of time is apparent as concluded above, and on approaching saturation a plateau is reached which reduces the adsorption rate (Figure 3.1b).

### 3.2 Obtaining Adsorption Isotherms

Adsorption isotherms are experimentally obtainable quantities and a key parameter within polymer science. The experimental methods used for determining adsorption isotherms may be *indirect* or *direct*. This means that they can either be determined indirectly from conditions of the solvent continuum or directly from the actual adsorbed amount at a surface.

Indirect methods usually involve some spectroscopic method such as ultraviolet-visible (UV), nuclear magnetic resonance or infra red (FTIR) techniques. With these one measures the concentration of polymer in the solvent before and after adsorption to some surface.

Direct methods usually involve techniques such as neutron- or optical reflectometry, ellipsometry, quartz crystal microbalance (QCM) or surface enhanced Raman scattering. Because direct methods measure an absolute quantity, rather than a difference, these are inherently more accurate but may suffer from faulty results due to contaminations on the surface investigated.<sup>9</sup>

## Chapter 4

# Modelling of Polymers

### 4.1 Coarse Graining

A full atomistic polymer model which includes all molecular interactions in a non-equilibrium system may be computationally feasible on a small scale but is inadequate for large systems or simulations of long time scales. The number of interacting particles for a system where solvent molecules are modelled explicitly limits such simulations even with the computer power now available to scientists. This problem is often dealt with by *coarse graining*.<sup>15</sup> There is always a careful balance of the number of parameters to include in a model in relation to the investigated properties. If one includes too many details, the time needed to obtain results is often wasted on events which do not significantly affect the system, while not including enough details may fail in resolving vital properties, giving false predictions of the state of a system.

The main objective of coarse graining is to reduce the number of interactions in a system which is highly dependent on the number of particles. More specifically, for a polymer model a reduction in the number of particles can be made by replacing groups of atoms with *united atoms*, retaining the average size of the polymer and properties of the backbone. Furthermore, one may replace quantum-mechanical potentials by empirical (mean-field) potentials for the bond length, torsional and bond angles, along with non-bonded interactions of the polymer.<sup>16,17</sup>

Below, we examine the polymer model and interactions which were used throughout the work presented in this thesis. It should be noted that the chosen model is one of many possibilities and was implemented in this work due to its simplicity, well established behavior, and wide application.

## 4.2 General Approach

The work presented in this thesis is based on a coarse grained *bead-spring* off-lattice model to mimic the behavior of polymers immersed in a good solvent. Solvent molecules are not explicitly included in the model but the solvent is treated as a continuum. The polymer is represented by spherical beads connected via harmonic bonds which may contract or expand to accommodate energetic variations in the local environment. Furthermore, a harmonic potential was included to mimic intrinsic stiffness along the polymer, enabling us to model polymers of desired persistence length. Non-bonded interactions were taken into account through a soft repulsive potential, precluding overlap of beads. Finally, an external potential from a surface in the solution was applied when adsorption or desorption of polymers was modelled. The sum of these energetic contributions in our model can thus be represented as a total energy  $U$  according to

$$U = U_{nonbond} + U_{bond} + U_{angle} + U_{surf} \quad (4.1)$$

## 4.3 Polymer Interaction Potentials

The non-bonded bead-bead potential energy  $U_{nonbond}$  is assumed to be pair wise additive according to<sup>18</sup>

$$U_{nonbond} = \sum_{i < j}^N u(r_{ij}) \quad (4.2)$$

where  $r_{ij}$  denotes the distance between the interacting beads. The potential energy is given by a truncated and shifted Lennard-Jones (LJ) potential

$$u(r_{ij}) = \begin{cases} 4\varepsilon \left[ -\left(\frac{\sigma}{r_{ij}}\right)^6 + \left(\frac{\sigma}{r_{ij}}\right)^{12} + \frac{1}{4} \right], & r_{ij} \leq 2^{1/6}\sigma \\ 0, & r_{ij} > 2^{1/6}\sigma \end{cases} \quad (4.3)$$

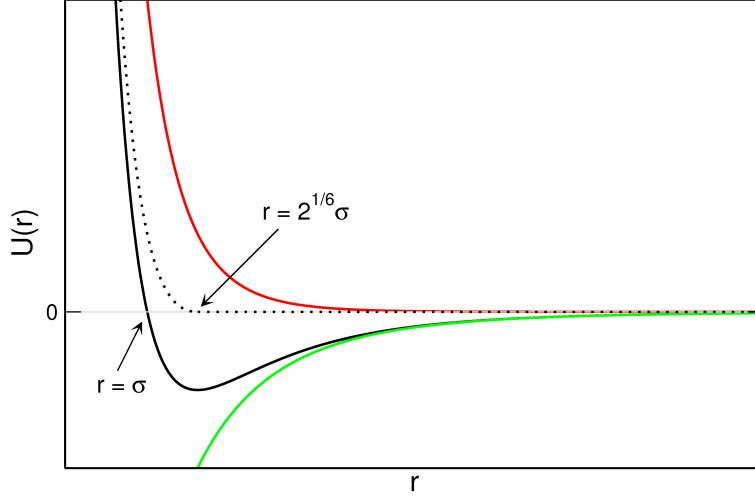


Figure 4.1: Lennard-Jones potential (solid black), shifted and truncated (dashed black), along with the attractive (green) and repulsive (red) contributions.

which describes the interaction between beads  $i$  and  $j$ , separated by the distance  $r_{ij}$ . Furthermore,  $\sigma$  is the diameter of the bead and  $\varepsilon$  is the interaction strength. The potential is constructed such that it is truncated at the minimum of the attractive part of the well occurring at  $r = 2^{1/6}\sigma$  and thereafter shifted to  $u(2^{1/6}\sigma) = 0$ , resulting in a smoothly increasing repulsion at short distances of interacting beads. In Figure 4.1 the LJ potential is schematically presented along with the truncated and shifted potential. The attractive and repulsive contributions of the potential is also displayed.

The bond interactions can be visualized as a spring with a variable stiffness which connects the beads along the polymer. The total contribution to the bond potential for  $N_p$  number of polymers of type  $\gamma$  is then given by

$$U_{bond} = \frac{1}{2}k_{bond} \sum_{p=1}^{N_{p,\gamma}} \sum_{i=1}^{N_{b,\gamma}-1} (r_{i,p} - r_{eq})^2 \quad (4.4)$$

where the the bond force constant  $k_{bond}$  regulates the stiffness of the spring and  $r_{eq}$  is the equilibrium distance between adjacent beads.

In a similar fashion,  $k_{angle}$  regulates the bond angle stiffness via

$$U_{angle} = \frac{1}{2} k_{angle} \sum_{p=1}^{N_{p,\gamma}} \sum_{i=2}^{N_{b,\gamma}-1} (\theta_{i,p} - \theta_{eq})^2 \quad (4.5)$$

where  $\theta_{eq}$  is the equilibrium bond angle. Again the summation is made over the number of polymers of a specific type.

#### 4.4 External Interaction Potentials

When polymers are modelled together with a surface there is a contribution to the total energy in the system by the  $u_{surf}$  term. The potential is also assumed pairwise additive

$$U_{surf} = \sum_{i=1}^N u_{surf}(z_i) \quad (4.6)$$

where  $z_i$  is the  $z$ -coordinate of a bead interacting with an attractive surface in the  $x, y$ -plane. Thus the summation is only dependent on the perpendicular coordinate of a bead. The completely smooth surface can be obtained by parallel integration of a crystalline surface of LJ-particles, including deeper layers. This yields an attractive 3-9 LJ potential of the form

$$u_{surf}(z_i) = \frac{2\pi}{3} \rho_s \sigma_s^3 \varepsilon_s \left[ - \left( \frac{\sigma_s}{z_i} \right)^3 + \frac{2}{15} \left( \frac{\sigma_s}{z_i} \right)^9 \right] \quad (4.7)$$

where  $\rho_s$  is the density of the LJ-particles with a mean diameter of  $\sigma_s$  in the crystalline surface. Once again the magnitude of the interaction is dependent on the potential energy parameter  $\varepsilon_s$ . The minimum of the attractive potential occurs at  $z_{min} = (2/5)^{1/6} \sigma_s$ , and at this distance the magnitude of the attraction amounts to  $u_{surf}(z_{min}) = -[2\pi(10)^{1/2}/9] \rho_s \sigma_s^3 \varepsilon_s \approx -2.2 \varepsilon_s$ .

In a similar way to the approach of eq 4.3, a soft repulsive potential can be produced from the attractive 3-9 LJ potential



$$u_{surf}(z_i) = \begin{cases} \frac{2\pi}{3} \rho_s \sigma_s^3 \varepsilon_s \left[ - \left( \frac{\sigma_s}{z_i} \right)^3 + \frac{2}{15} \left( \frac{\sigma_s}{z_i} \right)^9 + \left( \frac{\sqrt{10}}{3} \right) \right], & z_i \leq z_{min} \\ 0, & z_i > z_{min} \end{cases} \quad (4.8)$$

where the potential is truncated and shifted at the minimum of the attractive potential  $z_{min}$ .



## Chapter 5

# Statistical Thermodynamics

The following section is a very condensed summary on the foundations of statistical thermodynamics. For a more thorough introduction see standard textbooks on the subject.<sup>19–21</sup>

### 5.1 The Boltzmann Distribution and Entropy

Imagine a collection (*ensemble*) of  $\mathcal{N}$  macroscopically identical subsystems (same number of particles and same volume) which is isolated at a temperature  $T$ . The entire collection of subsystems is thus a representation of a thermodynamic system with the volume  $V$  and  $N$  particles, which has a total energy  $E$ . For any single subsystem, the energy states can be listed  $(\varepsilon_1, \varepsilon_2, \varepsilon_3, \dots)$  and are shared among all  $\mathcal{N}$  subsystems and are equally probable. At any instant there will be a number of subsystems  $(n_1, n_2, n_3, \dots)$  found in some energy state, e.g.,  $n_1$  number of subsystems in state  $\varepsilon_1$ , and so on. This imposes the following constraints on the system

$$\sum_j n_j = \mathcal{N} \quad (5.1)$$

$$\sum_j n_j \varepsilon_j = E \quad (5.2)$$

The weight of a configuration is given by the number of states  $\Omega$  of the ensemble for a given distribution according to

$$\Omega(n) = \frac{(n_1 + n_2 + \dots)!}{n_1! n_2! \dots} = \frac{\mathcal{N}}{\prod_j n_j!} \quad (5.3)$$

The distribution which has the largest value of  $\Omega$  will thus represent the most probable. It turns out that the most probable distribution is overwhelmingly large in comparison with the other distributions. The probability distribution depends on the energy of the state in accordance with the Boltzmann distribution:

$$P_j(N, V, T) = \frac{n_i}{\mathcal{N}} = \frac{e^{-\beta \varepsilon_i}}{Q(N, V, T)} \quad (5.4)$$

where

$$Q(N, V, T) = \sum_j e^{-\beta \varepsilon_j} \quad (5.5)$$

and  $\beta = 1/k_b T$ , the inverse of the temperature times the Boltzmann constant. The quantity  $Q(N, V, T)$  is referred to as the *canonical ensemble partition function*, from which all thermodynamic properties of a system can be calculated. We now define the entropy associated with the probability of the largest distribution according to

$$S(N, V, T) = -k_B \sum_j P_j \ln P_j \quad (5.6)$$

For a given observable  $\mathcal{A}$  in the limit as  $\mathcal{N} \rightarrow \infty$ , we obtain the average as a sum over all states with their associated weights as an ensemble average

$$\langle \mathcal{A} \rangle = \frac{\sum_j \mathcal{A} e^{-\beta \varepsilon_j}}{Q} \quad (5.7)$$

where the average of the mechanical property  $\mathcal{A}$  becomes the true ensemble average as the number of subsystems  $\mathcal{N}$  approaches infinity.

## 5.2 Classical Statistical Mechanics

The connection between statistical mechanics and quantum mechanics becomes evident in the classical limit where  $(k_B T \gg \Delta \varepsilon)$ .<sup>19</sup> As a

consequence, the sum over the energy levels is replaced by an integral in the partition function. At any given point in time, a set of particles in a system may be described by their position  $(\mathbf{x}_1, \dots, \mathbf{z}_N)$  and momenta  $\mathbf{p}_{\mathbf{x}1}, \dots, \mathbf{p}_{\mathbf{z}N}$ . For a set of  $N$  particles this gives a  $6N$  dimensional space, called the *phase space*. The total energy of the system can be described by the *Hamiltonian*  $\mathcal{H}$ , in which the contribution of the potential and kinetic energy is separated

$$\mathcal{H}(r, p) = \sum_i \frac{p_i^2}{2m} + U(x_1, \dots, z_N) \quad (5.8)$$

where  $m$  is the mass of the particle. For a system of interacting particles in a given volume  $V$ , the classical partition function becomes

$$\frac{1}{N!h^{3N}} \int e^{-\mathcal{H}(r,p)\beta} dx_1 \dots dp_{zN} \quad (5.9)$$

where the  $N!$  shows that the particles are indistinguishable and  $h$  is Planck's constant, which ensures that each quantum state is associated with a phase space volume. The momentum part of the integral  $\sum_i \frac{p_i^2}{2m}$  in eq 5.8 becomes

$$\int e^{-\mathcal{H}(p)\beta} dp_{x1} \dots dp_{zN} = \frac{1}{N!\Lambda^{3N}} \quad (5.10)$$

where  $\Lambda = (h^2/2(\pi mk_B T))^{(1/2)}$ . The classical partition function is then only a function of the positions of the particles according to

$$Q = \frac{1}{N!\Lambda^{3N}} \int_V e^{-U(x_1 \dots z_N)\beta} dx_1 \dots dz_N \quad (5.11)$$

In analogy with eq 5.7 we find for the classical statistical ensemble average for an observable  $\mathcal{A}$

$$\langle \mathcal{A} \rangle = \frac{\int \mathcal{A}(x_1 \dots z_N) e^{U(x_1 \dots z_N)\beta} dx_1 \dots dz_N}{\int e^{U(x_1 \dots z_N)\beta} dx_1 \dots dz_N} \quad (5.12)$$

which is now a  $3N$  dimensional integral. Despite the reduction, analytical results for such a statistical mechanical problems are few. Either further simplifications need to be made or alternative numerical methods used in order to solve this kind of problem. The next chapter will give some insight to numerical approaches to obtaining results to this kind of average.

## Chapter 6

# Molecular Simulation Techniques

This chapter will in short present some of the simulation techniques used throughout the work in this thesis. All simulations carried out in this work were done using the integrated software package MOLSIM©, which has been developed by Per Linse and co-workers at the Division of Physical Chemistry at Lund University.<sup>22</sup>

### 6.1 Motivation

Due to the complex nature of interactions in many-particle systems, analytical solutions to various properties are unobtainable. Simulation techniques such as Monte Carlo, molecular dynamics, and Brownian dynamics, can be used to predict thermodynamic and transport properties of a system by numerical calculations based on the interactions between modelled species. Simulation can thus be employed to validate a proposed model system by comparing its properties with experiments, and if there is agreement between the two a correct estimate of intermolecular interactions may be assumed. Furthermore, a simulation may be helpful in predictions of approximate analytical theory applied to the same model. The theory may then be adjusted until satisfactory results are achieved.

With increasing computer power the size and complexity of simulated systems increase. However, dynamics of non-equilibrium properties of polymers such as those studied in this work comprise rather heavy calculations. The longer Brownian dynamic simulation times presented in this work were in the order of 2000 CPU hours on 3.0 Ghz dual core processors. We used a simple model and therefore focused more on the

universal properties of the system rather than carrying out a quantitative study.

There are numerous comprehensive textbooks on the subject of simulation techniques,<sup>15,17,23,24</sup> which more specifically deal with the underlying concepts, theory, and algorithms needed. The following is a very limited and condensed description of Monte Carlo and Brownian dynamics simulation techniques.

## 6.2 Monte Carlo Simulation

The Monte Carlo (MC) simulations used in this work are based on the Metropolis algorithm, which is basically a weighted sampling method which probes the configurational part of the phase space introduced in section 5.2. The method relies on the use of a *Markov chain* to generate a set of states for a system, implying that (i) a state is only dependent on its immediately preceding state, and that (ii) there is a finite number of such states.<sup>26</sup> Furthermore, at equilibrium the condition of *detailed balance* must be met, meaning that the number of transitions *from* the equilibrium state *to* some other state exactly cancel each other. If this condition is not met the system may be brought out of equilibrium.

For each transition of a system the energy of the new state is calculated. The energy difference from the preceding state is evaluated and if the energy of the new state is lower the new state is accepted. If the energy of the new state is higher, however, the state may only be accepted on a partially random basis.

The following algorithm shows in six steps how a trial transition from one state to another is conducted for a system of  $N$  particles characterized by their coordinates  $\mathbf{r}_i = [x_i, y_i, z_i]$  and a maximum displacement parameter  $\delta$ :

1. Pick a particle  $i$  at random and pick three random numbers  $\eta_1, \eta_2, \eta_3$  in the interval  $[0,1[$ .
2. Calculate the new positions of the particle

$$\begin{aligned} x_i^{new} &= x_i^{old} + (2\eta_1 - 1)\delta \\ y_i^{new} &= y_i^{old} + (2\eta_2 - 1)\delta \\ z_i^{new} &= z_i^{old} + (2\eta_3 - 1)\delta \end{aligned}$$

3. Calculate the energy difference between the new and old positions of the particle:  $\Delta U = U_{new} - U_{old}$



4. If the energy of the new configuration is decreased ( $\Delta U > 0$ ) then accept the move and replace the old coordinates:  $\mathbf{r}_i^{new} = \mathbf{r}_i^{old}$ . Then update the energy:  $U_{new} = U_{old} + \Delta U$
5. If the energy is increased ( $\Delta U < 0$ ), pick another random number  $\eta_4$  on the interval  $[0,1[$ , and evaluate the following:

$\eta_4 < e^{-\beta\Delta U}$ : accept the move, update positions and energy.

$\eta_4 > e^{-\beta\Delta U}$ : reject the move, leave position and energy unchanged.

6. Pick another particle at random and proceed again according to steps 1 through 6.

The non-deterministic nature of the MC algorithm suggests that there is no inherent time coupling to relaxation toward equilibrium, making this method a poor choice for sampling of dynamic properties. However, such methods do exist and are commonly used.<sup>17</sup>

## 6.3 Brownian Dynamics Simulation

The natural choice of simulation method which incorporates the full dynamics of a system would be one which models time-dependent motion of all (relevant) molecular components, including individual solvent molecules. Such detailed methods exist and are commonly referred to as *molecular dynamics* (MD) simulations. Basically, these simulations numerically solve Newton's equations of motion using the position of a particle and the force which acts upon it, often using the Lagrangian formalism.<sup>25</sup> This is then carried out in a sequential manner for all particles, whereafter averages of desired properties are calculated for the system. However, when the process studied takes place on time scales which are much longer than the motion of the individual solvent molecules this is a poor choice.

Using Brownian dynamics (BD) simulation techniques has the advantage of not explicitly modelling the solvent molecules, but instead replacing these with stochastic forces which mimics their collective erratic motion. Once the rapid motion of the solvent molecules has been replaced by a stochastic force, time scales do not have to be resolved below that of the dynamics of the macromolecules, making simulations of macroscopic proportions computationally feasible. For a more complete

introduction into the physics of stochastic processes see textbooks on the subject.<sup>26,27</sup>

A stochastic equation which describes a system represents a number of possible realizations, all with an associated probability. In a Brownian dynamics simulation individual realizations are chosen in such a way that the time evolution of the system provides the correct probability distribution. The stochastic equation is integrated forward in time to create trajectories which describe the motion of a particle suspended in solution. The equation of motion (used in this work) for the simple case of no external flow, assumed incompressible flow, and no hydrodynamic interactions becomes<sup>17,28</sup>

$$\mathbf{r}_i(t + \Delta t) = \mathbf{r}_i(t) + \frac{D_0 \Delta t}{kT} \mathbf{F}_i(t) + \mathbf{R}_i(t; \Delta t) \quad (6.1)$$

where  $\mathbf{r}_i(t + \Delta t)$  is the location of particle  $i$  at the time  $t + \Delta t$ ,  $\mathbf{r}_i(t)$  the location of particle  $i$  at the time  $t$ ,  $D_0$  the particle self-diffusion coefficient in the absence of systematic forces,  $k$  Boltzmann's constant,  $T$  the temperature, and  $\mathbf{F}_i(t)$  the systematic force on particle  $i$  at time  $t$  arising from the potential energy in the system. Furthermore,  $\mathbf{R}_i(t; \Delta t)$  is a random displacement of bead  $i$  representing the effect of collisions with solvent molecules at time  $t$  and is sampled from a Gaussian distribution with the mean  $\langle \mathbf{R}_i(t; \Delta t) \rangle = 0$  and the variance  $\langle \mathbf{R}_i(t; \Delta t) \cdot \mathbf{R}_j(t'; \Delta t) \rangle = 6D_0 \Delta t \delta_{ij} \delta(t - t')$  as obtained from the fluctuation-dissipation theorem. The theorem regulates the interrelation between the stochastic and deterministic terms in the stochastic differential equation, ensuring that all fluxes at equilibrium must be zero, maintaining a detailed balance.

Different techniques have been developed which have more or less of the elements associated with Brownian dynamics but also of molecular dynamics. The common notion, however, is to consider these as Brownian dynamics as long as the solvent in the model is treated as a continuum.

## 6.4 Boundary conditions

As pointed out in section 5.1, true values of any calculated mechanical property are valid in the limit of infinite number of subsystems. Clearly the number of simulated particles in any system is much lower than this and thus still very far from the validity of the thermodynamic limit. It can in other words not be assumed that the confinement of a

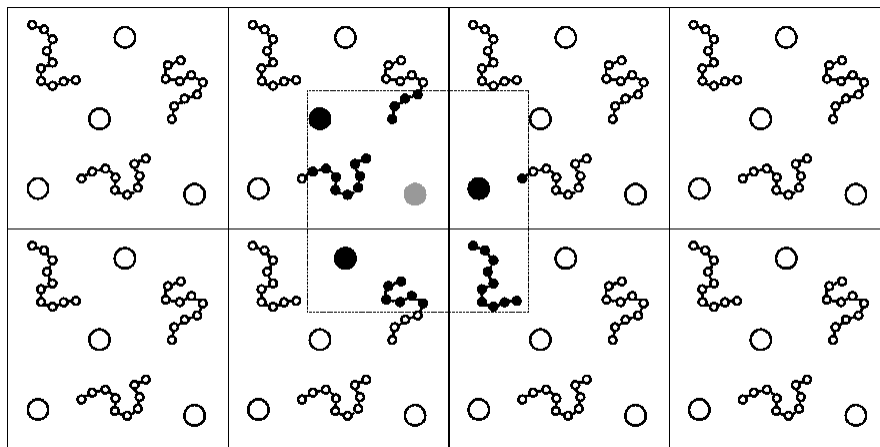


Figure 6.1: Schematic representation of boundary conditions for a system of polymers and particles. Interacting entities (black) to a central (gray) particle are displayed.

system within a given volume may not effect the outcome of a calculated property.

The need to simulate bulk behavior is essential in any system and is usually achieved by the implementation of *periodic* boundary conditions. This means that any particle in a system interacts on the length scale of the entire system, as depicted in Figure 6.1. In other words, any chosen particle in a given system will interact with its surrounding as if it were localized in the center of the system at all times.

Boundary conditions may be combined in a simulation so that some directions are periodic in nature while others do not allow periodicity. This may be invoked for example when simulating the adsorption onto a solid surface which is modelled along one of the coordinate axes.

## 6.5 Truncation and Neighbor Lists

Another important technical aspect is that of the number of interactions in an  $N$ -particle system. Calculating the potential of interaction between particles in such a system implies the evaluation of  $N(N - 1)/2$  pair interactions. This means that the time needed to evaluate the energy of the system scales as  $N^2$ . If a system of short-ranged interactions is

simulated there is a high probability that a substantial amount of CPU-time is devoted to pair interactions which do not significantly contribute to the total energy of the system.

It is obvious that the efficiency of the simulation may be increased by excluding interactions at some distance  $r_c$ . At distances larger than  $r_c$ , the potential is then *cutoff*, either by a simple truncation or a truncation and shift. In molecular or Brownian dynamics simulations, the latter choice of handling the potential is preferred, as forces on the particles are finite. The magnitude of  $r_c$  must of course be chosen with great care and one must be aware of implications of introducing cutoffs to the potential. For example, a correctional pressure term may be needed for simple truncations and an energy tail contribution may be needed when there is a truncation and shift.

Reducing the number of pair interaction calculations does not reduce the number of  $N(N - 1)/2$  pair distance evaluations. This problem can, however, also be approached by introducing *neighbor lists*. The neighbor list is implemented by introducing a second cutoff distance  $r_v > r_c$ , which is schematically shown in Figure 6.2. Before the interactions are calculated, a list is made of all particles within the distance  $r_v$  of particle  $i$ . As long as the displacement of particle  $i$  is smaller than  $r_v - r_c$  there is no need to update the neighbor list. Every time the neighbor list is updated the calculation remains in the order of  $N^2$ . However, when the neighbor list is used the calculation is in the order of  $N$  for a large number of particles. The efficiency of the neighbor list method depends on the

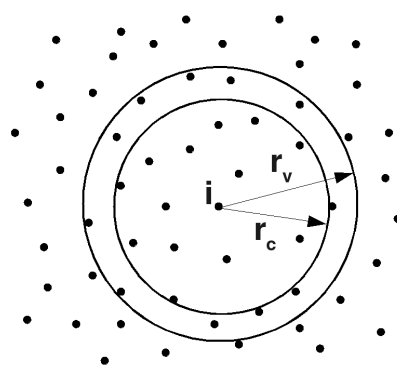


Figure 6.2: Schematic representation of the implementation of neighbor list. Particle  $i$  interacts with particles within the cutoff  $r_c$ , while the neighbor list contains all particles within  $r_v$ .

number of particles which need to be listed. This should be significantly smaller than the total number of particles in the system.

## 6.6 Simulation Protocol

The simulations performed in Paper I - IV involve both MC and BD methods. The MC simulations were used for the generation of equilibrium configurations of (i) single polymers in Paper I, and (ii) polymer solutions in Paper II - IV. In this section the employed protocols which enabled simulations of the two different situations will in the following be presented briefly.

In the single polymer studies presented in Paper I, the following simulation protocol was employed:

- i Equilibrium conformations of polymers with desired length and stiffness were generated in a cubic simulation box of length  $L_x = L_y = L_z$ , with periodic boundary conditions applied in  $x$ ,  $y$ , and  $z$ -directions.
- ii After the initial generation and relaxation, the polymer was translated in the  $z$ -direction to a position in the box where the closest bead-to-surface distance was fixed at a distance  $z_s$ .
- iii An adsorbing surface was invoked in the  $x, y$ -plane, using the 3-9 LJ potential described in eq 4.7, after which the BD simulation was started.
- iv A time limit was set at which the polymers must have attached to the bare surface. If this criteria was not met the simulation was disregarded.

Steps i - iv were repeated  $\approx 1000$  times for each polymer type and averages of desired properties were continuously collected during the simulation.

The desorption studies in the same paper were conducted in a similar manner:

- i Equilibrium adsorbed structures of polymers were generated with applied potential using the 3-9 LJ potential.
- ii The potential was truncated and shifted according to eq 4.8, yielding a soft repulsive potential at the surface, after which the BD simulation were initiated.

The average properties were evaluated in the same way as in the adsorption studies described above.

The use of MC simulations to create initial equilibrium properties was also utilized in Paper II - IV where adsorption from solutions of polymers was studied. The protocol in these simulations involved the following:

- i Generation and equilibration of a bulk solution containing polymers of desired type in a simulation box of lengths  $L_x = L_y = L'_z$ , where  $L'_z = L_z + \Delta_z$ . Periodic boundary conditions were applied in the  $x$  and  $y$ -directions, whereas in the  $\pm z$ -direction hard walls were invoked at  $\pm L_z/2$ . This created a slab of polymer free zone adjacent to the surfaces located at  $\pm L'_z/2$ .
- ii The hard walls were removed, and the 3-9 LJ was invoked at  $\pm L'_z/2$ , after which the BD simulation was started.

Sampled properties were averaged over both surfaces ( $\pm L'_z/2$ ).

## 6.7 Sampled Properties

One important issue that remains, is what properties to examine once we have a working simulation method applied to a model system, whether it is in equilibrium or not.

The simplest, and maybe most relevant property due to the applicability is that of the adsorbed amount of polymer  $\Gamma$ . This property is conceptually easy to grasp, where we need only define a parallel plane in relation to the adsorbing surface where a polymer may be considered to be adsorbed. However, one must bear in mind the unphysical and nontrivial choice of such a definition of adsorption. Furthermore, in comparison with an experimental setup, the polymer bulk density is often insensitive to adsorption, which may not be the case in a simulation. The property is nonetheless important in our study as it enables us to determine the adsorption rates, attachment and detachment processes and equilibrium adsorbed amounts for our systems. We adopt the notation of  $N_b^{ads}$  for the number of adsorbed beads and  $N_p^{ads}$  for the number of adsorbed polymers. Furthermore, the same quantity may be expressed in terms of surface density profiles, either as the surface density of beads  $\rho_b$  or  $\rho_p$  polymers.

The location of a polymer as a function of time during an adsorption is described by its center of mass  $r_{com}(t)$ , which was defined in eq 2.11. The time-dependent analog of this property then becomes

$$\langle \mathbf{r}_{com}(t) \rangle = \left\langle \frac{1}{N} \sum_{i=1}^N \mathbf{r}_i(t) \right\rangle \quad (6.2)$$

where  $\mathbf{r}_i(t) = [x_i(t), y_i(t), z_i(t)]$  is the coordinate of bead  $i$  at time  $t$ . Specifically the location of a polymer's center of mass perpendicular to the surface along the  $z$ -axis,  $\langle z_{com}(t) \rangle$ , is of interest and obtained by replacing  $\mathbf{r}_i(t)$  with  $z_i(t)$  in eq 6.2.

As previously discussed in section 2.3, the radius of gyration  $R_g$  is a useful measure when it comes to describing the three-dimensional structure of a polymer. This property may also be followed as a function of time using

$$\langle R_g^2(t) \rangle = \left\langle \frac{1}{N} \sum_{i=1}^N [\mathbf{r}_i(t) - \mathbf{r}_{com}(t)]^2 \right\rangle \quad (6.3)$$

At sufficient bead-surface interaction strength, an adsorbing polymer will make a transition from a three-dimensional structure in solution to a more pancake-like two-dimensional structure at the surface. The adsorption will not only induce a collapse perpendicular to the surface but will also increase the expansion of the polymer parallel to the surface due to excluded volume interactions between adsorbed beads. This rearrangement of a polymer was monitored using the perpendicular ( $\perp$ ) and parallel ( $\parallel$ ) components of  $\langle R_g^2(t) \rangle$  according to

$$\langle R_g^2(t) \rangle_{\perp} = \left\langle \frac{1}{N} \sum_{i=1}^N [z_i(t) - z_{com}(t)]^2 \right\rangle \quad (6.4)$$

$$\langle R_g^2(t) \rangle_{\parallel} = \left\langle \frac{1}{N} \sum_{i=1}^N \{[x_i(t) - x_{com}(t)]^2 + [y_i(t) - y_{com}(t)]^2\} \right\rangle \quad (6.5)$$

satisfying  $\langle R_g^2(t) \rangle = \langle R_g^2(t) \rangle_{\perp} + \langle R_g^2(t) \rangle_{\parallel}$ .

As a polymer becomes adsorbed, its adapted structure at the surface may be described by loop, tail, and train subchains.<sup>9</sup> A subchain of

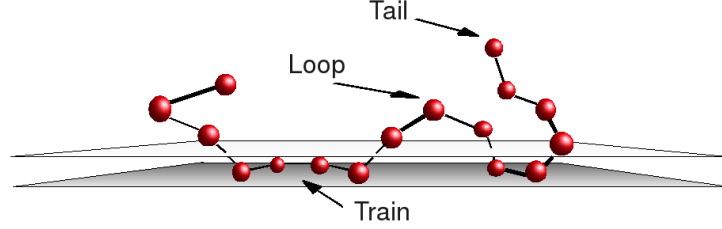


Figure 6.3: Schematic representation of the three different kinds of subchains. The plane which defines a bead as adsorbed is also shown.

adsorbed beads is referred to as a train, a non-adsorbed subchain with both ends bonded to trains as a loop and a non-adsorbed subchain with one end bonded to a train as a tail, as depicted in Figure 6.3. The definition of an adsorbed polymer depends on where the adsorption plane is placed parallel to the surface; the plane is then used to define the different types of subchains.

During the adsorption of nonflexible polymers, these tend to form nematic structures on the surface, where the degree of nematic order is much dependent on the persistence length of the polymer. In Paper III and IV, we evaluate the nematic bond order by considering the bond order parameter  $\eta$ , which is evaluated in the proximity of an adsorbed bond  $i$  as

$$\eta_i = \lambda_i \quad (6.6)$$

where  $\lambda_i$  is the largest eigenvalue of the 3x3 matrix  $\mathbf{B}_i$ , in which the elements are defined by

$$\mathbf{B}_{\alpha\beta,i} = \frac{1}{N_{V_i}} \sum_{j \in V_i} \frac{1}{2} (3\mathbf{b}_{\alpha,j}\mathbf{b}_{\beta,j} - \delta_{\alpha\beta}) \quad (6.7)$$

where  $\mathbf{b}_j$  is the normalized bond axis vector of bond  $j$ ,  $\{\alpha, \beta\} = \{x, y, z\}$  and the summation involves  $N_{V_i}$  bonds in the spherical volume  $V_i$  with the radius  $R_\eta$  centered at bond  $i$ . Only bonds that are adsorbed are included in the sum; thus, in practice bonds in a cylinder of radius  $R_\eta$  and a height given by the adsorption threshold ( $z$ -axis) are considered.



---

The bond order parameter ranges from zero for random bond directions to unity for completely parallel bond directions. The formation of structured domains on the surface is analyzed by studying the time-dependent bond order  $\eta(t)$ .



## Chapter 7

# Highlights of the Papers

Here the results from paper I - IV will briefly be discussed and the main conclusions of the work will be highlighted.

### 7.1 Paper I

The simplest case of adsorption of polymers using our model is the adsorption of single polymers onto a solid surface from a good solvent. The focus is thus a comparison to a polymer solution in the dilute regime, where the polymers behave uninfluenced by other polymers in the solution. In paper I, we examined the behavior of single polymers as these adsorb onto a planar surface as a function of time. The properties varied were (i) the polymer length, (ii) intrinsic polymer stiffness, and (iii) the polymer-surface interaction strength.

During the adsorption of polymers we identified three distinct phases corresponding to periods during the adsorption of significant conformational change. The phases were as follows:

- **Distortion phase**, where the polymers become elongated perpendicular to the surface as the segments closest to the surface experience an attraction.
- **Attachment phase**, where the polymers establish physical contact with the surface, which is followed by a relatively fast collapse of the polymer to a more two-dimensional structure.
- **Relaxation phase**, where the polymers continue to spread on the surface attaining their equilibrium structure. The relaxation involves essentially only the parallel extension on the surface and comprises the slowest process.

We identified the characteristic time of the attachment phase for the polymers as a function of the polymer length  $N$ , which revealed a sub-linear behavior, whereas the relaxation phase revealed a much stronger  $N$  dependence. The result reflects the polymer's geometrical size in solution, and the fact that as it collapses onto the surface there will be an increasing entanglement of segments of a polymer with  $N$ .

Increasing the stiffness of the polymers promoted a flatter conformation on the surface at equilibrium, which could also be induced with a stronger bead-surface interaction. Furthermore, the attachment phase was reduced and the relaxation was prolonged for polymers with a higher surface affinity. For a stiffer polymer, the process of attachment differs as there is a preferential realignment for the stiffer polymers rather than a collapse of a flexible object.

## 7.2 Paper II

In our second contribution, we extended the system to investigate solutions of flexible polymers with varying density and polymer length. We found that the collective diffusion of the polymers toward the surface is enhanced by higher bulk density, as well as the relaxation on the surface in terms of formation of subchains.

The relaxation of the number of adsorbed polymers toward the equilibrium value was investigated in some detail. Comparisons to a solution of adsorbing unconnected beads revealed a biexponential behavior corresponding to that of the polymer solutions. This was attributed to the (i) adsorption to a bare surface and (ii) to a surface which is partly covered.

We also investigated the rate and frequency of attachment and detachment of the polymers at the surface. From this we concluded some general aspects related to the polymer length and the density of the solution. (I) Lower densities of shorter polymers showed a correlation between early attaching polymers and those that remain attached for a long time of the simulation. (II) Higher densities of shorter polymers showed virtually no such correlation but an increasing and higher reattachment frequency of polymers at the surface. (III) Longer polymers which adsorb early showed a higher frequency in reattachment than polymers adsorbing late during the simulation.

The relaxation of the polymers on the surface revealed yet another process than those obtained in Paper I. During the structural relaxation, the increased surface pressure induces a final contraction of polymers parallel to the surface reducing the polymer fraction of beads in trains and increasing the fraction in tails.

### 7.3 Paper III

In Paper III we conducted a comprehensive survey on polymer adsorption from solution, varying the intrinsic polymer stiffness and the bead-surface interaction strength. The work comprised both static and dynamic investigations of the systems.

We found an interesting dependence of the average number of adsorbed polymers and the average number of adsorbed beads on the flexibility of the polymers. At any given bead-surface interaction strength, there is a maximum in the average number of adsorbed polymers when the flexibility of the polymers is initially decreased. This was only observed for slightly nonflexible polymers, and was attributed to the competing effects of the larger perpendicular extension of polymers, as a result of increased surface pressure, and the preferred parallel adsorption of a rod-like polymer.

The adsorption rates of flexible and rod-like polymers are initially similar, but the final relaxation of the property is prolonged for the latter. Our analysis shows that this longer relaxation occurs as a consequence of the slow formation of domains with nematic bond order on the surface. The process appears on time scales comparable to that of the entire simulation, and thus constituting the slowest relaxation mechanism.

Finally, we conducted an analysis by which we extracted information of mean integration times of polymers into the adsorbed layer along with average adsorption times. The flexible polymers displayed increasing integration times and average adsorption times with increasing bead-surface interaction strength. This is an effect of a higher bead density at the surface as the bead-surface interaction is increased, creating a less penetrable barrier for non-adsorbed polymers arriving at the surface which increases the time needed for a polymer to become firmly anchored. For the rod-like polymers these times increased 3-fold as compared to flexible polymers at equal bead-surface attraction, as a consequence of the higher surface affinity of these polymers. When a rod-like polymer is adsorbed at the surface this occurs with an average fraction of 60 to 80 % of the polymer in trains depending on the bead-surface attraction.

Therefore, the probability that all of these segments are simultaneously detached is smaller than for flexible polymers with fewer segments in trains. This explains the large increase both in integration times and adsorption times.

## 7.4 Paper IV

In Paper IV, having established much of the dynamic processes which occur for one-component solutions in Paper II and III, we introduced mixed solutions of polymers with varying degree of rigidity, polymer length, and bead-surface interaction strength. We aimed to resolve some of the dynamic competitive events during the co-adsorption of different types of polymers.

Regarding the number of adsorbed beads for the flexible polymers, the general dynamic behavior that we captured during the simulations well resembled those of several experimental systems previously studied. We identified certain time-dependent events regarding the competitive adsorption which distinguished the mixed systems from adsorption of the single component solutions. These were:

- a reduction of the number of adsorbed beads compared to the respective polymer types single component solution; this effect was more pronounced for the shorter polymer.
- a maximal number of adsorbed beads was reached for the shorter polymer at the same time as the longer polymer revealed a markedly slower adsorption rate.
- a slow exchange of the shorter for longer polymer types at the surface, occurring at constant number of adsorbed beads.

The different combinations of stiff and flexible polymer lengths revealed that the stiff and long polymers dictate the adsorption behavior in terms of the number of adsorbed beads at the surface. However, for a mixture of flexible long polymers and stiff short ones, the shorter polymers replaced the long at the surface. This induced an overadsorption of the longer polymers, prolonging the subsequent replacement of these by the short stiff ones.

# Populärvetenskaplig sammanfattning på svenska

Polymerer är långa kedjemolekyler som består av sammanhängande mindre repeterande enheter. Vi finner dessa nästan överallt; vi har dem i håret när vi tvättar oss, i maten vi äter, i förpackningar, i medicin och i rengöringsmedel. Kroppen producerar långa komplicerade former av polymerer som proteiner och styrs via den kanske viktigaste polymeren av alla, vår arvs massa - DNA. I många tekniska applikationer vill man kontrollera, antingen genom att tillåta eller genom att förhindra, polymerer från att fästa vid olika ytor. Detta har gjorts i flera hundra år och görs fortfarande i stor utsträckning på basis av empiriska försök. Vill man förstå vad som sker eller kanske vad som inte sker måste man förstå de bakomliggande mekanismerna i en sådan process. Detta är viktigt när det gäller att ta fram nya material med skräddarsydda egenskaper.

Avhandlingsarbetet har fokuserat på några av de tidsberoende processer som sker då en eller flera olika polymerer fäster vid ytor. De processer som sker i en lösning där en polymer närmar sig en yta, för att sedan fästas och spridas på denna, sker ofta på mycket korta tidsskalor och det är svårt att experimentellt studera sådana processer. Därför använder vi olika typer av matematiska modeller och numeriska metoder för att simulera dessa förlopp. De modeller vi använder för att representera polymerer, lösningsmedel och ytor anpassas till en detaljnivå som är hanterbar, men ändå representativ. Simuleringarna går ut på att numeriskt lösa de ekvationer som beskriver systemets energitillstånd och hur de olika polymererna växelverkar med sin omgivning. Eftersom vi i modellen har konstruerat en lägre potential invid den yta som vi vill att polymererna skall fästa på, kommer de tids nog också att hamna där. Det måste också finnas en någorlunda riktig tidsskala om vi vill hävda att de olika processerna tar olika tid och förstå varför de gör det. Detta har vi löst med hjälp av den specifika simuleringsmetod vi använt: Brownsk dynamik. Metoden innebär att det lösningsmedel

som innehåller polymererna och själva ytan har egenskaper som till viss del liknar de fysikaliska betingelser hos vanligt vatten. Istället för enskilda vattenmolekyler skapar man en helhet som omsluter polymererna och kontinuerligt ger dem knuffar i slumpmässiga riktningar. Det finns regler för hur lösningsmedlet delar ut knuffar och däri ligger också tidsberoendet.

De olika system vi har tittat på innefattar polymer med olika längd, stelhet och attraktionskraft till ytan. I vårt första arbete undersökte vi ensamma polymerer när dessa fäster vid en yta; detta för att kartlägga och isolera de tidsberoende processer som råder beroende på systemets karaktär. Efterföljande arbeten behandlar lösningar med flera polymerer, dels av samma slag, men också blandsystem av olika polymertyper. Dessa arbeten visar på de effekter som uppstår då flera polymerer täcker en yta och hur detta kan påverka den enskilda polymerens struktur. I de fall där det handlar om olika typer av polymerer uppstår det konkurrens om plats intill och på ytan. Det kan ta mycket lång tid för dem att arrangera sig för att nå jämvikt. I vissa fall kan stela polymerer uppvisa olika mönster på ytan i samband med att de täcker denna, så kallade nematiska tillstånd, vilket också bidrar till mycket långa tider för att nå jämvikt.

Även om de förlopp vi har studerat inte riktar sig specifikt mot någon speciell typ av polymer eller system, så ligger värdet av resultaten i de kvalitativa egenskaper som vi har kartlagt. De processer vi har studerat för polymerer och ytor beskriver således generella egenskaper och sätter dessa i relation till varandra i tiden. Detta gör att förståelsen för de fenomen vi har modellerat kan appliceras och utvecklas för andra system och polymertyper och kan då även jämföras med experimentella resultat.



# References

1. Grosberg, A. Yu.; Khokhlov, A. R. *Giant Molecules: Here, There, and Everywhere...*; Academic Press, USA, 1997.
2. Grosberg, A. Yu.; Khokhlov, A. R. *Statistical Physics of Macromolecules*; AIP Press, New York, 1994.
3. de Gennes, P-G. *Scaling Concepts in Polymer Physics*; Cornell University Press, London, 1979.
4. Doi, M.; Edwards, S. F. *The Theory of Polymer Dynamics*; Oxford University Press, Belfast, 1989.
5. Evans, D. F.; Wennerström, H. *The Colloidal Domain: Where Physics, Chemistry, Biology and Technology Meet* 2ed; Wiley-VCH, New York, 1999.
6. O'Shaughnessy, B.; Vavylonis, D. *J. Phys. Condens. Matter* 2005, 17, R63.
7. Norde, W. *Colloids and Interfaces in Life Sciences*; Marcell Dekker, Inc., New York, 2003.
8. Fleer, G. J.; Lyklema, J. In *Adsorption From Solution at the Solid/Liquid interface*; Academic Press: New York, 1983.
9. Fleer, G. J.; Cohen Stuart, M. A.; Scheutjens, J. H. M. H.; Cosgrove, T.; Vincent, B. *Polymers at interfaces*; Chapman & Hall: London, 1993.
10. Jönsson, B.; Lindman, B.; Holmberg, K.; Kronberg, B. *Surfactants and Polymers in Aqueous Solution*; John Wiley & Sons Ltd., West Sussex, 1998.
11. Cohen, M. A.; de Keizer, A. *Oxide Surfaces, Surfactant Science Series 103*; Marcell Dekker, Inc., New York, 2001.

12. Cohen Stuart, M. A.; Fleer, G. J. *Annu. Rev. Mater. Sci.* 1996, 26, 463
13. Cohen Stuart, M. A. *Surfactant Science Series* 2003, 110, 1.
14. Yethiraj, A. *Adv. Chem. Phys.* 2002, 121, 89.
15. Frenkel, D.; Smit, B. *Understanding Molecular Simulation*; Elsevier, USA, 2002
16. Baschnagel, J.; Mayer, H.; Varnik, F.; Metzger, S.; Aichele, M.; Müller, M.; Binder, K.; *Interface Science* 2003, 11, 159
17. Binder, K. *Monte Carlo and Molecular Dynamics Simulations in Polymer Science*; Oxford University Press, USA, 1995.
18. Israelachvili, J. *Intermolecular & Surface Forces*; Elsevier, San Diego, 2005.
19. Hill, T. L. *An Introduction to Statistical Thermodynamics*; Dover Publications, New York, 1986.
20. Chandler, D. *Introduction to Modern Statistical Mechanics*; Oxford University Press, USA, 1987.
21. Kjellander, R. *The Basis of Statistical Thermodynamics*; Lecture notes, 2001.
22. MOLSIM, Version 4.0, Linse, P.; Lund University, Sweden, 2004.
23. Allen, M. P.; Tildesley, D. J. *Computer Simulations of Liquids*; Oxford University Press: Oxford, England, 1987.
24. Leach A. R. *Molecular Modelling: Principles and Applications*; Pearson Education Limited, 1999.
25. Goldstein, H. *Classical Mechanics* second ed. Addison-Wesley Publishing Company, Inc., USA, 1980.
26. Gardiner, C. W. *Handbook of Stochastic Methods for Physics, Chemistry and the Natural Sciences* second ed. Springer Verlag, Berlin, 1994.
27. Leons, D. S. *An Introduction to Stochastic Processes in Physics*; The John Hopkins University Press, Maryland, 2002.
28. Ermak, D. L.; McCammon, J. A. *J. Chem. Phys.* 1978, 69(4), 1352.